

Isolation, Structure, and Electronic Calculations of the Heterofullerene Salt $K_6C_{59}N$

Kosmas Prassides,* Majid Keshavarz-K.,
Jan Cornelis Hummelen, Wanda Andreoni, Paolo Giannozzi,
Ernst Beer, Cheryl Bellavia, Luigi Cristofolini, Rosario González,
Alexandros Lappas, Yasuo Murata, Magdalena Malecki,
Vojislav Srdanov, Fred Wudl*

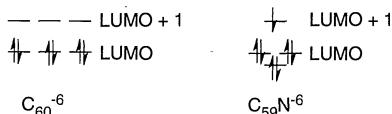
An intercalation compound of azafullerene, $K_6C_{59}N$, was prepared and structurally characterized. It is isostructural with the fullerene compound K_6C_{60} , adopts a body-centered-cubic structure (lattice constant $a = 11.31$ angstroms), and consists of quasi-spherical monomeric $(C_{59}N)^{6-}$ ions. Density functional calculations of the structural and electronic properties confirm the similarity to K_6C_{60} but also suggest a sizable deformation, principally confined in the vicinity of the nitrogen atom, of both the molecular structure and the electron states. These results show that study of the intercalation chemistry of azafullerene promises to reveal a rich family of both *n*- and *p*-doped systems with novel conducting and magnetic properties, like their fullerene antecedents.

When $(C_{59}N)_2$ was isolated, its potential as a structural, but not electronic, analog of C_{60} was discussed (1). The C_{60} molecule has a triply degenerate t_{1u} lowest unoccupied molecular orbital (LUMO), which, when half-filled with electrons from alkali metal atoms, gives rise to metallic A_3C_{60} salts with half-filled electronic bands, face-centered-cubic (fcc) structures, and, at ambient pressure, transitions to the superconducting state in the range of 2 to 33 K (2–4). When the t_{1u} level is completely filled, the stoichiometry requires six alkali metal ions (A_6C_{60}), the resistivity once again reaches a maximum, and the resulting insulating salts adopt a body-centered-cubic (bcc) structure (5).

In the case of the $C_{59}N$ molecule, as a result of the lower symmetry, the t_{1u} triplet LUMO is no longer degenerate (6–8). Moreover, because of the trivalency of nitrogen versus the tetravalency of carbon, the neutral molecule is an open shell with partial occupancy of one of the t_{1u} levels, which has reduced energy:



Complete filling of the levels arising from the t_{1u} manifold should require, in principle, only five alkali metal atoms, as shown below. Thus, reduction of $C_{59}N$ with six electrons necessitates population of the LUMO + 1 state:



Here, we report that the $C_{59}N$ dimer, $(C_{59}N)_2$ (1), the crystal structure of which

is still unknown (9), reverts to a monomer upon doping with excess K metal. The saturation product, whose stability is possibly driven by its large Madelung energy (10), is isostructural with K_6C_{60} and has a stoichiometry $K_6C_{59}N$ and a bcc crystal structure. Supporting ab initio optimization of the structure and electron energy-band calculations on $K_6C_{59}N$ suggest the likelihood of an ionic metal, whereas comparison with its fullerene analog reveals sizable but localized structural and electronic changes.

Heating $(C_{59}N)_2$ (~5 mg) with excess K, in Pyrex capillary tubing at 250°C for 36 hours under vacuum in a sealed tube, yielded a free-flowing, crystalline powder. The K-filled capillary was kept at the cooler (by ~10°C) end of the evacuated tube at all times. Two rather unusual physical properties of as-prepared $(C_{59}N)_2$ (11) are that it has a tendency to adhere to surfaces and is difficult to grind into a fine powder. An x-ray diffraction (XRD) pattern of the sample (after a subsequent 24-hour annealing at 250°C) sealed in a glass capillary 0.5 mm in diameter was recorded at ambient temperature with a Siemens D5000 diffractometer ($2\theta = 5^\circ$ to 45° , wavelength $\lambda = 1.5406$ Å). Data analysis was performed with the PROFIL (12) suite of Rietveld analysis programs, with the background modeled by linear interpolation. Preliminary susceptibility measurements with a SQUID (superconducting quantum interference device) susceptometer on the same sample revealed no evidence of superconductivity. We performed structural optimization and calculation of the electron energy bands in the frame of density functional theory in the local density approximation (LDA), following the approach that had been suc-

cessfully applied to other fullerides (13). We used norm-conserving pseudopotentials, a plane-wave basis set for the expansion of the electronic wave functions with an energy cutoff of 55 rydbergs, and the P point as representative of the Brillouin zone for the electron density. The lattice constant was fixed at the experimental value, and the molecules were kept in the T_h orientation as in (13). Hence, the results are directly comparable with those for K_6C_{60} . Comparisons can also be made with analogous calculations on molecular $C_{59}N$ (6, 7), so that the effect of N substitution for C can be distinguished from that of K doping.

Inspection of the XRD profile (shown as dots in Fig. 1) reveals that all reflections index to bcc symmetry. Moreover, their intensities are in remarkable correspondence with those observed in the fullerene analog K_6C_{60} (3, 5). Rietveld refinements of the profile were thus attempted in space group $Im\bar{3}$ with the K^+ ions occupying the distorted tetrahedral positions at $(0, 0.5, z)$ ($z = 0.2890 \pm 0.0007$ Å). We modeled the azafulleride $(C_{59}N)^{6-}$ ions by using orientationally ordered C_{60} molecules in which all C–C distances were kept fixed at 1.44 Å (Fig. 2), in analogy with the Rietveld refinement of K_6C_{60} . The refinement converged rapidly ($R_{wp} = 0.151$, $R_1 = 0.118$, $R_{exp} = 0.101$, background excluded) with a cubic lattice constant $a = 11.313 \pm 0.004$ Å [$a(K_6C_{60}) = 11.39$ Å]. The center-to-center distance between neighboring azafulleride ions was 9.80 Å, somewhat smaller than the average interdimer distance in both the pristine azafullerene (9.97 Å) and K_6C_{60} (9.86 Å). Refinement of the K occupation number always indicated full stoichiometry ($n = 6$) within one estimated standard deviation. The calculated fit and the difference profile are shown in Fig. 1. High-resolution synchrotron XRD or neutron diffraction patterns would be necessary to allow refinement of the individual C positions and identification of the unique N position and any associated local distortion.

K. Prassides, Institute for Polymers and Organic Solids, Departments of Chemistry and Materials, University of California, Santa Barbara, CA 93106, USA, and School of Chemistry and Molecular Sciences, University of Sussex, Falmer, Brighton BN1 9QJ, UK.

M. Keshavarz-K., J. C. Hummelen, E. Beer, C. Bellavia, R. González, Y. Murata, M. Malecki, V. Srdanov, F. Wudl, Institute for Polymers and Organic Solids, Departments of Chemistry and Materials, University of California, Santa Barbara, CA 93106, USA.

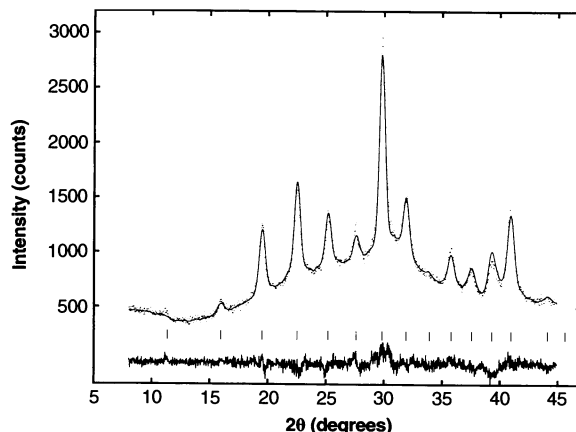
W. Andreoni, IBM Research Division, Zürich Research Laboratory, 8803 Rüschlikon, Switzerland.

P. Giannozzi, Scuola Normale Superiore, I-56126 Pisa, Italy, and IBM Research Division, Zürich Research Laboratory, 8803 Rüschlikon, Switzerland.

L. Cristofolini and A. Lappas, School of Chemistry and Molecular Sciences, University of Sussex, Falmer, Brighton BN1 9QJ, UK.

*To whom correspondence should be addressed.

Fig. 1. The upper curve shows the final observed (points) and calculated (solid line) diffraction profile for $K_6C_{59}N$ at room temperature in the range of $2\theta = 8^\circ$ to 45° (Cu $K\alpha$ radiation). The lower panel shows the difference profile. Vertical marks indicate the observed reflections.



Inasmuch as the XRD powder pattern of the saturation-doped K heterofulleride does not allow differentiation from its fulleride analog, the unlikely possibility that $C_{59}N$ had somehow been converted to C_{60} under strongly reductive conditions needed to be explored. To this end, a sample of $K_6C_{59}N$ was undoped with methanolic *p*-toluenesulfonic acid (the acid acts as an oxidant, presumably releasing H_2). High-performance liquid chromatography analysis showed that $C_{59}NH$ and $(C_{59}N)_2$ were produced, but not C_{60} .

Intercalation with alkali metals causes marked relaxation of the C_{60} molecule (13), leading in particular to a lengthening of the short C–C bonds as a result of the excess electrons that are occupying orbitals with antibonding character. Using the $C_{59}N$ molecule as a reference (6, 7), we found that the LDA calculations on the azafulleride also reveal the same effect and are consistent with full ionic character for the $K_6C_{59}N$ salt. In addition, the K^+ ions occupy similar sites in the fulleride and azafulleride salts, in agreement with the XRD results.

The results of the band structure calcu-

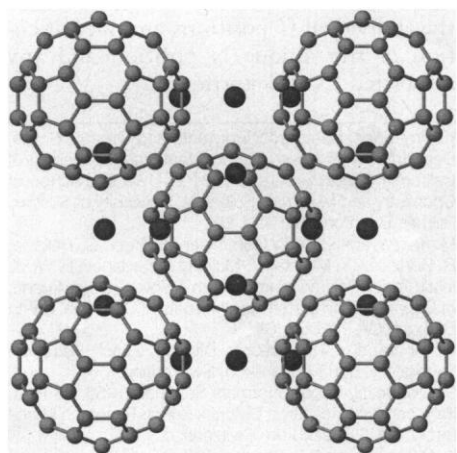


Fig. 2. Unit-cell basal plane projection of the bcc structure of $K_6C_{59}N$. The location of the N atom on the azafulleride ion is currently unknown.

lations for $K_6C_{59}N$ are shown in Fig. 3A and can be compared with those for K_6C_{60} (Fig. 3B). In contrast to the insulating behavior of K_6C_{60} (band gap ~ 0.8 eV), $K_6C_{59}N$ is predicted to be metallic. The effect of spin polarization on the half-filled band of $K_6C_{59}N$ is not considered here. However, spin polarized calculations of $C_{59}N$ (7) show that spin polarization effects are only slight, leading to an energy splitting of ≤ 0.1 eV. In Fig. 3A, the values at the Γ point essentially represent the one-electron levels of the $C_{59}N$ molecule to which six electrons have been added. The main effect evident for the specific molecular orientation chosen here is the large splitting of the lowest t_{1u} -derived level (0.3 eV), which localizes strongly in

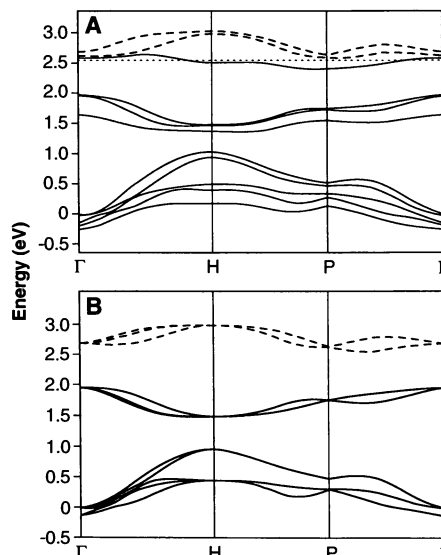


Fig. 3. Kohn-Sham electron energy bands of (A) $K_6C_{59}N$ and (B) K_6C_{60} along some symmetry lines of the Brillouin zone of the bcc crystal. $E = 0$ corresponds to the top of the h_u -derived bands of C_{60} at the $k = 0$ (Γ) point. The other bands (above $E = 0$) are those derived from the t_{1u} levels (solid lines, $E = 1.5$ to 2 eV) and t_{1g} levels (solid and dashed lines, $E = 2.5$ to 3 eV). The dotted line in (A) represents the estimated value for the Fermi level.

the vicinity of the N atom, as shown in Fig. 4. However, the t_{1g} -derived levels are almost unaffected by the presence of N at $k = 0$, but are significantly modified along the (1,0,0) line (Γ –H). In fact, the one-electron state at H has the same localization pattern as that shown in Fig. 4.

The successful synthesis of the azafulleride salt $K_6C_{59}N$ —which is isostructural with its analog K_6C_{60} , with essentially unchanged lattice dimensions and the K^+ ions occupying the same distorted tetrahedral interstices in the bcc arrangement of $(C_{59}N)^{6-}$ ions—opens the way for the isolation of a new family of alkali metal azafulleride salts. The theoretical results reveal local structural changes and non-rigid-band behavior in the transition from C_{60} to $C_{59}N$ and from K_6C_{60} to $K_6C_{59}N$. However, as the modifications are spatially localized, the overall effects on the π -delocalized states of C_{60} are minor. The structural similarity of $K_6C_{59}N$ with C_{60} salts should likely prevail for other members of the $A_nC_{59}N$ ($A =$ alkali metal) series, but the electronic difference between $C_{59}N^{n-}$ and C_{60}^{n-} that arises from the extra electron should sensitively affect the conducting, magnetic, and electronic properties of the materials. Furthermore, the availability of azafulleride salts should also prove crucial for the theoretical understanding of the electronic structure and properties of superconducting fullerides and for the testing of various proposed scenarios. The most interesting cases should be those of the $KC_{59}N$ salt, in which the extra electron should fill the state that is most affected by the presence of the nitrogen atom (Fig. 4), and of the

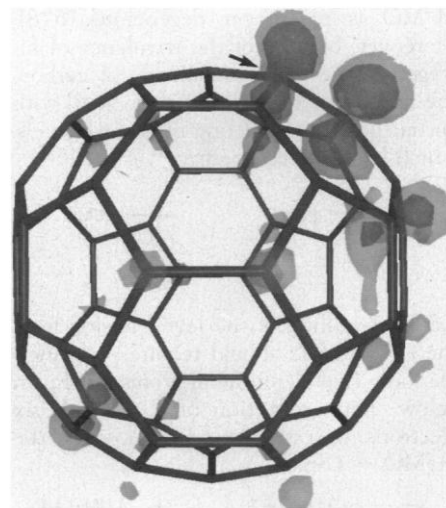


Fig. 4. Probability density of the lowest of the t_{1u} -derived states at Γ at ~ 1.6 eV in Fig. 3A, which is most affected by the replacement of a C atom by N. The light and dark areas correspond to $e/au^3 = 0.005$ and 0.01, respectively. The arrow points toward the N atom.

$K_2C_{59}N$ salt, which is isoelectronic with the K_3C_{60} superconducting phase.

REFERENCES AND NOTES

- J. C. Hummelen, B. Knight, J. Pavlovich, R. González, F. Wudl, *Science* **269**, 1554 (1995).
- R. C. Haddon *et al.*, *Nature* **350**, 320 (1991).
- R. M. Fleming *et al.*, *ibid.* **352**, 787 (1991).
- K. Tanigaki *et al.*, *ibid.*, p. 222.
- O. Zhou *et al.*, *ibid.* **351**, 462 (1991).
- W. Andreoni, F. Gygi, M. Parrinello, *Chem. Phys. Lett.* **190**, 159 (1992).
- W. Andreoni, unpublished results.
- R. C. Haddon, personal communication.
- The XRD measurements of as-prepared solid $(C_{59}N)_2$ reveal at ambient temperature a mostly amorphous solid with a minority hexagonal ($a = 9.97$ Å, $c = 16.18$ Å) crystalline phase (K. Prassides *et al.*, in preparation).
- Y. Wang, D. Tománek, G. F. Bertsch, R. S. Ruoff, *Phys. Rev. B* **47**, 6711 (1993).
- The material also has a remarkable tendency to self-assemble into large hollow spherical particles, as evidenced by extensive scanning electron microscope and transmission electron microscope studies (9).
- J. K. Cockcroft, *Program PROFIL* (Birkbeck College, London, 1994).
- W. Andreoni, P. Giannozzi, M. Parrinello, *Phys. Rev. B* **51**, 2087 (1994).
- We thank an anonymous reviewer for bringing (10) to our attention. Supported in part by the MRL program of NSF under award DMR-91-23048 and grant DMR-9500888. Financial support was also provided by the Engineering and Physical Sciences Research Council (UK).

1 November 1995; accepted 5 January 1996

The Elasticity of a Single Supercoiled DNA Molecule

T. R. Strick, J.-F. Allemand, D. Bensimon, A. Bensimon, V. Croquette

Single linear DNA molecules were bound at multiple sites at one extremity to a treated glass cover slip and at the other to a magnetic bead. The DNA was therefore torsionally constrained. A magnetic field was used to rotate the beads and thus to coil and pull the DNA. The stretching force was determined by analysis of the Brownian fluctuations of the bead. Here, the elastic behavior of individual λ DNA molecules over- and underwound by up to 500 turns was studied. A sharp transition was discovered from a low to a high extension state at a force of ~ 0.45 piconewtons for underwound molecules and at a force of ~ 3 piconewtons for overwound ones. These transitions, probably reflecting the formation of alternative structures in stretched coiled DNA molecules, might be relevant for DNA transcription and replication.

The supercoiling of DNA—that is, the twisting and bending of the double helical axis—is an extensively studied aspect of DNA topology (1, 2). It affects both structural transitions and interactions between DNA and other molecular complexes. For example, a locally underwound DNA strand is necessary for transcriptional activation (3) and recombinational repair (4). Supercoiled DNA is also a key structural factor in chromosomal organization, in which the winding of the molecule around histone proteins is necessary for DNA compaction (5). More specifically, the entropic tension generated in supercoiled DNA in anaphase during chromosomal condensation is released by the action of a specific enzyme (6), topoisomerase II, thus allowing the disentanglement and segregation of the chromosomes necessary before cell division.

Most previous studies of DNA supercoiling were done on solutions of circular supercoiled DNA molecules with the use

of dynamic light-scattering methods (7), fluorescence depolarization (8), and topoisomer analysis during the circularization of small DNA molecules (9–12). Among the studies on single molecules are the analysis of static electron microscopy images of small plasmids (13–15) and Monte-Carlo (MC) or molecular dynamics simulations (16–19). Most of these experiments have been interpreted on the basis

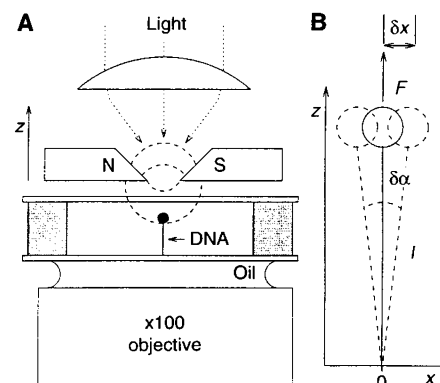
of models of DNA that assume that the twisting and bending contributions to the free energy of the molecule are harmonic and isotropic (20–22), a good approximation for unstretched DNA (8–12).

For closed circular DNA and for linear DNA molecules whose ends are not free to rotate (6), topological models provide the conceptual framework (2, 13) we shall use to analyze our data. The number of times the two strands of the DNA double helix are intertwined—the linking number of the DNA (Lk)—is a topological constant, the sum of two geometrical characteristics of the shape of the DNA, writhe (Wr) and twist (Tw), where $Lk = Wr + Tw$ (2). Wr is a measure of the coiling of the DNA axis, like a twisted cord forming interwound structures (plectonemes). Tw reflects the helical winding of the DNA strands around each other (13). For an unconstrained (relaxed) linear DNA molecule (assuming the absence of any spontaneous local curvature), $Lk = Lk_0 = Tw_0$ (= number of helical turns). One defines the relative change in linking number or degree of supercoiling, σ , as

$$(Lk - Lk_0)/Lk_0 \equiv \Delta Lk/Lk_0$$

The value of σ for most circular molecules

Fig. 1. (A) Experimental setup: The DNA molecule was bound to a glass cover slip at one end by DIG-anti-DIG links and at the other end to a paramagnetic bead by biotin-streptavidin links (26, 27). A force was applied on the bead with Co-Sm magnets equipped with a polar piece to focus the field in a 2-mm gap located just above the sample. The magnetic device can spin about the optical axis, causing the paramagnetic beads to rotate. We controlled the magnitude of the force by displacing the magnets vertically. To determine this force, we measured the Brownian fluctuations and the coordinates of the tethered bead. The samples were observed on a Diaphot-200 Nikon microscope with a 100 \times immersion oil objective. The x and y coordinates were directly measured on the image. The value of the z coordinate was obtained with an optical sensor to measure the position of the objective, which yielded the best image determined by a polynomial fit to the bead's profile. The Brownian motion of the tethered bead was measured in real time with a special tracking algorithm inspired by previous work (41). We obtained video data using a square pixel XC77CE Sony camera connected to a Cyclope frame grabber (timed on the pixel clock of the camera) installed in a 486 (33 MHz) personal computer (42). N and S represent the two poles of a magnet. **(B)** Schematic of a bead undergoing angular fluctuations ($\delta\alpha$) in the xOz plane transverse to the direction of stretching. The transverse restoring force is $F_{\perp} = F\delta\alpha = (F/l)\delta x$.



T. R. Strick, Laboratoire de Physique Statistique de l'ENS, associé aux universités Paris VI et VII, 24 rue Lhomond, 75231 Paris Cedex 05, and Laboratoire de Biophysique de l'ADN, Institut Pasteur, 25-28 rue du Dr Roux, 75015 Paris, France.

J.-F. Allemand, D. Bensimon, V. Croquette, Laboratoire de Physique Statistique de l'ENS, associé aux universités Paris VI et VII, 24 rue Lhomond, 75231 Paris Cedex 05, France.

A. Bensimon, Laboratoire de Biophysique de l'ADN, Institut Pasteur, 25-28 rue du Dr Roux, 75015 Paris, France.